𝒟𝐼-𝟥𝐼-𝟢𝒟

Docket No. 58077/JPW/JSG

# IN THE UNITED STATES PATENT AND TRADEMARK OFFICE

ASSISTANT COMMISSIONER FOR PATENTS
Washington, D.C. 20231

January 27, 2000

S I R :

Transmitted herewith for filing are the specification and claims of the patent application of:

Anna Marie Pyle and Eckhard Jankowsky _____ for
Inventor(s)

ASSAYS FOR EVALUATING THE FUNCTION OF RNA HELICASES _____
Title of Invention

Also enclosed are:

__X__  __8__ sheet(s) of ____ ·informal __X__ formal drawings.

____ Oath or declaration of Applicant(s).

____ A power of attorney

____ An assignment of the invention to _____

_____

____ A Preliminary Amendment

__X__ A verified statement to establish small entity status under 37 C.F.R. §1.9 and §1.27.

The filing fee is calculated as follows:

### CLAIMS AS FILED, LESS ANY CLAIMS CANCELLED BY AMENDMENT

|  | NUMBER FILED |  | NUMBER EXTRA* |  | RATE | | | FEE | |
|---|---|---|---|---|---|---|---|---|---|
|  |  |  |  |  | SMALL ENTITY | OTHER ENTITY |  | SMALL ENTITY | OTHER ENTITY |
| TOTAL CLAIMS | 8 – 20 | = | 0 | X | $ 9 | $ 18 | = | $ 0 | $ — |
| Independent Claims | 3 – 3 | = | 0 | X | $ 39 | $ 78 | = | $ 0 | $ — |
| Multiple Dependent Claims Presented:  __X__ Yes ____ No |  |  |  |  | $ 130 | $260 | = | $ 130 | $ — |
| * If the difference in Col. 1 is less than zero, enter "0" in Col. 2 |  |  |  |  | BASIC FEE | | | $ 345 | $ 760 |
|  |  |  |  |  | TOTAL FEE | | | $ 475 | $ — |

__X__    A check in the amount of $ __475.00__ to cover the filing fee.

_____    Please charge Deposit Account No._____ in the amount of $_____.

__X__    The Commissioner is hereby authorized to charge any additional fees which may be required in connection with the following or credit any over-payment to Account No. __03-3125__;

      __X__  Filing fees under 37 C.F.R. §1.16.

      __X__  Patent application processing fees under 37 C.F.R. §1.17.

      _____  The issue fee set in 37 C.F.R. §1.18 at or before mailing of the Notice of Allowance, pursuant to 37 C.F.R. §1.311(b).
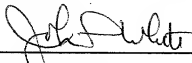
__X__    Three copies of this sheet are enclosed.

_____    A certified copy of previously filed foreign application No. _____ filed in _____ on _____. Applicant(s) hereby claim priority based upon this aforementioned foreign application under 35 U.S.C. §119.

__X__    Other (identify)   Express Mail Certificate of Mailing bearing Label

                                 No.: EL 086 014 857 US, dated January 27, 2000.

                                 One loose set of formal drawings.

Respectfully submitted,

John P. White
Registration No. 28,678
Attorney for Applicant(s)
Cooper & Dunham LLP
1185 Avenue of the Americas
New York, New York 10036
(212) 278-0400

VERIFIED STATEMENT (DECLARATION) CLAIMING
SMALL ENTITY STATUS UNDER 37 C.F.R. §1.9(f)
AND §1.27(d) - NONPROFIT ORGANIZATION

I hereby declare that I am an official empowered to act on behalf of the nonprofit
organization identified below:

Name of Organization: __The Trustees of Columbia University in the City of New York__

Address of Organization: __110 Low Memorial Library, West 116th Street & Broadway,__
__New York, New York 10027__

TYPE OF ORGANIZATION:

    __X__     UNIVERSITY OR OTHER INSTITUTION OF HIGHER EDUCATION
          TAX EXEMPT UNDER INTERNAL REVENUE SERVICE CODE 26 U.S.C. §§501(a) and
          501(c)(3)
          NONPROFIT SCIENTIFIC OR EDUCATIONAL UNDER STATUTE OF STATE OF THE UNITED
          STATES OF AMERICA
          NAME OF STATE: _____
          CITATION OF STATUTE: _____
          WOULD QUALIFY AS TAX EXEMPT UNDER INTERNAL REVENUE SERVICE CODE 26 U.S.C.
          §§501(a) and 501(c)(3) IF LOCATED IN THE UNITED STATES OF AMERICA
          WOULD QUALIFY AS NONPROFIT SCIENTIFIC OR EDUCATIONAL UNDER STATUTE OF STATE
          OF THE UNITED STATES OF AMERICA IF LOCATED IN THE UNITED STATES OF AMERICA
          NAME OF STATE: _____
          CITATION OF STATUTE: _____

I hereby declare that the nonprofit organization identified above qualifies as a
nonprofit organization as defined in 37 C.F.R. §1.9(e)* for purposes of paying
reduced fees under 35 U.S.C. §41(a) and 41(b), with regard to the invention entitled
__ASSAYS FOR EVALUATING THE FUNCTION OF RNA HELICASES__

by inventor(s)__ Anna M. Pyle and Eckhard Jankowsky__

described in:

    __X__     the specification filed herewith
          application serial no. _____ filed _____
          patent no. _____ issued _____

I hereby declare that rights under contract or law have been conveyed to and remain
with the nonprofit organization with regard to the above identified invention.

If the rights held by the nonprofit organization are not exclusive each individual,
concern, or organization known to have rights to the invention is listed below[a] and
no rights to the invention are held by any person, other than the inventor, who could
not qualify as a small business concern under 37 C.F.R. §1.9(d)* or a nonprofit
organization under 37 C.F.R. 1.9(e)*

[a]NOTE: Separate verified statements are required from each person, concern, or
organization having rights to the invention averring to their status as small
entities. 37 C.F.R. §1.27.

Name:    __N/A__
Address: _____

      ____Individual     ____ Small Business Concern     ____Nonprofit Organization

*See Reverse

Small Entity/Nonprofit
Page -2-

Applicants: Anna M. Pyle and Eckhard Jankowsky
Serial No.: Not Yet Known
Filed: Herewith

I acknowledge the duty to file, in this application or patent, notification of any
change in status resulting in loss of entitlement to small entity status prior to
paying, or at the time of paying, the earliest of the issue fee or any maintenance fee
due after the date on which status as a small entity is no longer appropriate. 37
C.F.R. §1.28(b)*.

I hereby declare that all statements made herein of my own knowledge are true and that
all statements made on information and belief are believed to be true; and further
that these statements were made with the knowledge that willful false statements and
the like so made are punishable by fine or imprisonment, or both, under 18 U.S.C.
§1001, and that such willful false statements may jeopardize the validity of the
application, any patent issuing thereon, or any patent to which this verified
statement is directed.

Name of Person Signing:   Mr. Jack M. Granowitz
Title In Organization:    Executive Director, Columbia Innovation Enterprise
Address: Amsterdam & 120th Street - Suite 363 New York, New York 10027

Signature: 
Date Of Signature:        1/26/00

*See Reverse

*Application*
*for*
*United States Letters Patent*

**To all whom it may concern:**

   Be it known that      **Anna Marie Pyle and Eckhard Jankowsky**

have invented certain new and useful improvements in

## ASSAYS FOR EVALUATING THE FUNCTION OF RNA HELICASES

of which the following is a full, clear and exact description.

## Assays For Evaluating
## The Function Of RNA Helicases

### Background on the Invention

Throughout this application, various publications are referenced by author and date. Full citations for these publications may be found listed alphabetically at the end of the specification immediately preceding Sequence Listing and the claims. The disclosures of these publications in their entireties are hereby incorporated by reference into this application in order to more fully describe the state of the art as known to those skilled therein as of the date of the invention described and claimed herein.

RNA conformation is of elemental importance in RNA-induced catalysis, as well as RNA interactions with other cellular components. Many central components of gene expression and RNA metabolism occur in large ribonucleoprotein complexes, most notably the ribosome and spliceosome. Within these large complexes, alternative conformations of specific RNAs have been demonstrated and the alteration of RNA conformation is believed to play a critical role in enabling, driving and assuring the fidelity of the catalytic reactions these complexes perform (Staley and Guthrie, 1998). Therefore, understanding the factors capable of inducing RNA conformational alterations within these complexes is likely to be central to an overall appreciation of

mechanisms by which they execute their intricate and demanding functions.

By exploring the effect of the duplex length of the substrates on the unwinding reaction under defined reaction conditions, the response of unwinding rate and amplitude to the duplex length can provide information about processivity and directionality (Fig. 1). Thus, the requirements for an experimental setup to probe and quantify processivity and directionality are to develop a substrate system where only the duplex length is variable and, using this substrate system, establish experimental conditions where rate and/or amplitude provide information about processivity and directionality.

RNA helicases of the DExH/D family play an essential role in viral replication and cellular RNA metabolosim, including central functions in RNA splicing, translation and regulation of gene expression. Despite the importance of these proteins, their RNA helicase activity has not been subjected to enzymological study. Basic knowledge of cellular metabolism is therefore constrained by a limited understanding of reaction mechanism by motor proteins in the RNA helicase family. To address this problem, mechanistic studies have been initiated on two viral DExH/D proteins which are part of the RNA helicase family: NPH-II from Vaccinia and NS3-4A from Hepatitis C Virus (HCV). The NPH-II protein is shown to be a processive, directional RNA helicase with specific roles for both the binding and hydrolysis of ATP. Having established qualitative features of NPH-II activity, the use of direct and stopped-flow kinetic methods to determine the quantitative kinetic parameters such as

translocation rates, reaction step size, processivity, helicase binding, ATP binding and hydrolic rate constants that describe the framework for catalytic activity of this prototypical RNA helicase. All aspects of cellular RNA metabolism and processing involve DExH/D proteins, which are a family of enzymes that unwind or manipulate RNA in an ATP-dependent fashion (de la Cruz, et al., 1999). DExH/D proteins are also essential for the replication of many viruses, and therefore provide targets for the develpment of therapeutics (Radare and Haenni, 1999). All DExH/D proteins characterized to date hydrolyse neucleoside triphosphates and, in most cases, this activity is stimulated by the addition of RNA or DNA. Several members of the family unwind RNA duplexes in an NTP dependent fashion *in vitro* (de la Cruz, et al., 1999 and Wagner, et al., 1998); therefore it has been proposed that DExH/D proteins couple NTP hydrolysis to RNA conformational change in complex macromolecular assemblies (Stanley and Guthric, 1998). Despite the central role of DExH/D proteins, their mechanism of RNA helicase activity remains unknown. It is shown that the DExH protein NPH-II unwinds RNA duplexes in a processive, unidirectional fashion with a step size of roughly one-half helix turn and that there is a quantitative connection between ATP and helicase processivity, thereby providing direct evidence that DExH/D proteins can function as molecular motors on RNA.

## Summary of the Invention

The present invention provides a method for detecting the release of a single-stranded RNA from an RNA duplex which comprises: (a) admixing an RNA helicase with the RNA duplex under conditions permitting the RNA helicase to unwind the RNA duplex and release single-stranded RNA, wherein the RNA duplex comprises a first RNA having a first label attached thereto and a second RNA, such first label being capable of producing a luminescent energy pattern when the first RNA is present in the RNA duplex which differs from the luminescent energy pattern produced when the first RNA is not present in the RNA duplex, (b) subjecting the admixture to conditions which permit (i) the RNA helicase to unwind the RNA duplex and release single-stranded RNA, and (ii) the first label to produce luminescent energy; and (c) detecting a change in the luminescent energy pattern produced by the first label so as to thereby detect release of single-stranded RNA from the RNA duplex.

## Breif Description of the Figures

### Figure 1

Kinetic approach to probe processivity and directionality of the unwinding reaction. Unwinding of a dsRNA is the reverse reaction of the association of two complementary ssRNAs. Thus, unwinding occurs only when so many basepairs are disrupted that no nucleation locus can form. Practically, that means that unwinding is only observed, when less then 4 or 3 basepairs remain in the duplex. This emphasizes that by monitoring a duplex unwinding reaction one actually monitors the very last event of the strand separation process.

A processive reaction occurs in distinct consecutive steps, therefore, there are reaction intermediates (I) until the reaction product (P) is formed. For a non-processive reaction (for instance if the unwinding occurs in one power stroke) there are no intermediates. Thus, the experimental rationale for probing processivity is to determine whether there are reaction intermediates or not. If the reaction proceeds in distinct consecutive translocation steps, the translocation is rate limiting for the unwinding reaction, and the rate constants ($k_{tr}$) of these translocation steps are of similar or equal size, intermediates (I) would accumulate. This would be reflected in a lag phase in the unwinding timecourse of the product (P) formation. With increasing duplex length more reaction intermediates would appear and timecourses would display a greater lag phase with increasing duplex length. The number of intermediates ($I_{1...n}$) is indicative for the number of kinetic steps that the helicase takes to unwind a duplex of given length. More intermediates cause also more dissociation "events", provided that these intermediates are susceptible to dissociation. This is

determined by the ratio of the translocation rate constant ($k_{tr}$) to the respective dissociation rate constant ($k_{di}$) (Ali and Lohmann, 1997). If a measurable fraction of protein dissociates during each unwinding step, the reaction amplitude should decrease with increasing duplex length. This should also occur when the translocation is not rate-limiting for the unwinding reaction. However, in that case the duplex length should not affect the reaction rate. If the reaction is not processive, there should be under no conditions a sensitivity of either reaction rate or amplitude to the length of the duplexes.

Probing the processivity is the prerequisite for testing the directionality of the unwinding, since only a processive reaction can be directional. The directionality can be directly tested by monitoring at least one reaction intermediate and the reaction product at the same time under conditions where the translocation limits the unwinding reaction. The experimental conditions for probing processivity and directionality have to be chosen in a way, that all RNA is complexed with protein at the reaction start and that all dissociation of the protein off the RNA substrate is irreversible.

**Figure 2**
Unwinding of various RNA substrates by NPH-II. Unwinding reactions were performed in a reaction buffer comprising $30\mu L$ volume (40mM Tris.Cl, pH 8.0, 2mM DTT, 20mM NaCl, 3mM $MgCl_2$, 3mM ATP, 16nM NPH-II, 3nM RNA substrate) at 23 C. Protein, RNA substrate, and $MgCl_2$ were incubated in reaction buffer prior to the reaction for 7 min. The reaction was started by addition of ATP. Aliquotes were

withdrawn at appropriate times and added to two volumes
quenching buffer (25mM EDTA, 0.4% SDS, 10% glycerol,
0.05% BPB, 0.05% XCB). This mixture was immediately
cooled on ice. After the last aliquot was taken, the
samples were applied to 15% native PAGE.

**Figure 3**

Effect of trap RNA on unwinding reactions. (A) Since
reactions are performed with preannealing of protein and
RNA prior to the reaction, the protein-RNA complex [ES]
is already formed at the reaction start. As protein
dissociates from the RNA substrate during the unwinding
reaction, re-binding of the protein and multiple reaction
cycles can occur. Binding ("trapping") free protein
during the course of unwinding prevents re-binding during
the reaction. Complete "trapping" of all free protein is
ensured by using a large excess of RNA (trap RNA) as
compared to the duplex substrate. (B) Effect of trap
addition on reactions with LS83 and LS36. Reaction
conditions were as described in Fig. 2, except that the
ATP was pre-mixed with the trap RNA (39-mer RNA oligo)
and the reaction was started with this ATP/trap mixture.
The trap concentration in the reaction was 600nM which is
an 200 fold excess over the substrate. Higher
concentrations of trap did not change the observed
timecourses. The substrate was bound to 100% of the
protein prior to the reaction as verified by gel shift
analysis of the RNA protein complexes (not shown).

**Figure 4**

Monitoring duplex unwinding by fluorescence energy
transfer. (A) Both strands of the duplex are labeled
with a fluorescence transfer donor-acceptor-pair of
fluorescent dyes. The top strand is labeled with

flourescein (donor) at the 3'-end and the bottom strand
is labeled with rhodamin (acceptor) at the 5'-end. The
attached fluorescein is excited at 492nm. Due to the
proximity of the acceptor label in the duplex, the
emission of the fluorescein label is quenched. Upon
unwinding, both labels depart from each other, the
quenching of the fluorescein label no longer occurs and
an increase in the emission of the fluorescein
fluorescence can be detected. (**B**) The unwinding
reactions were performed as described in Fig. 3, but in
a volume of 600µL in a fluorescene cuvette. The
fluorescence intensity was measured at defined intervals
(small points). The resulting curve was corrected for
the reaction amplitude derived by gel shift measurements
of identical reactions and both, the derived fluorescence
curve and the measurements from gel shift experiments
(large points) are overlaid in the plots. Reactions were
performed with US18 (18bp duplex region) and US36 (36bp
duplex region).

**Figure 5**

Effect of ATP concentration on the unwinding reaction.
Unwinding reactions with LS36 were performed as described
in Fig. 3 (pre-annealing, trap addition). The plot shows
the final amplitude of the reaction versus the respective
ATP concentration. Amplitude values were determined out
of 8 aliquotes taken from the reaction.

**Figure 6**

Effect of $Mg^{2+}$ substitution on the unwinding reaction.
Timecourses with US36 were measured as described in Fig.
3 (trap RNA, pre-annealing), except that 3nM $Mg^{2+}$ (**A**) was
substituted with 3mM $Mn^{2+}$ (**B**) and 3mM $Co^{2+}$ (**C**). The left
panels show the gel printouts of the reactions that are

plotted on the right panels as fraction unwound substrate versus time.

**Figure 7**

Effect of the duplex length on unwinding reactions in the presence of $Co^{2+}$. Unwinding reactions were performed with US36 (36bp duplex region) and US18 (18bp duplex region) under the conditions described in Fig. 6. The solid lines represent fits for a consecutive 2 step reaction with equal rate constants (Ali and Lohmann, 1997) for the 18bp duplex and for a consecutive 4 step reaction with equal rate constants for the 36bp duplex.

**Figure 8**

Probing the directionality of the unwinding reaction by using multi-piece substrates. **(A)** Multi-piece substrates were generated by site directed processing of the top strand RNA with an engineered DNAzyme (Santoro and Joyce, 1997) and subsequent hybridization of the two "pieces" with the bottom strand. **(B)** Unwinding reactions of MPS 36/75 (36nt oligo binds next to the single stranded overhang and 75nt oligo binds adjacent to this strand) and MPS 83/28 (83nt oligo binds next to the single stranded overhang and 28nt oligo binds adjacent to this strand) in the presence of $Mg^{2+}$ were carried out as described in Fig. 3. The fraction of the displaced pieces was calculated according to $frac[N]_t = [N_t / (N_t + M_t + S_t)] * [(N_\infty + M_\infty + S_\infty)/N_\infty]$, where $frac[N]_t$ is the fraction of the respective "piece" at the time t; $N_t$ is the intensity of the band of the "piece" N at the time t; $M_t$ is the intensity of the band of the "piece" M at the time t; $S_t$ is the intensity of the not unwound substrate band at the time t; $N_\infty$ is the intensity of the band of

the "piece" N after heat denaturation; $M_\infty$ is the intensity of the band of the "piece" M after heat denaturation and $S_\infty$ is the intensity of the not unwound substrate band after heat denaturation. $S_\infty$ is, however, usually zero. The solid lines represent a fit of the timecourse to a rate law describing a sum of two first order reactions. **(C)** Reactions of MPS 36/75 and MPS 83/28 in the presence of $Co^{2+}$ were performed as described in Fig. 6. The fraction of the displaced pieces were calculated as described above. The solid lines represent fits of the timecourses to rate laws describing a consecutive 4 step reaction for T36, a 12 step reaction for T75 and T28 and a 9 step reaction for T 83, using equal rate constants for the steps, respectively.

**Figure 9**

Kinetics of duplex unwinding. Reactions in the presence (open circles) and absence (filled circles) of trap RNA with a 36-bp substrate **(a)** and a 83-bp substrate **(b)**. The 83-bp substrate is an extension of the 36-bp substrate. The fraction of unwound substrate (indicated on the $y$ axis) was fitted to the integrated first-order rate law using Kaleidagraph software (Abelbeck). Rate constants (k) and reaction amplitudes (A) in the absence of trap RNA: k = 3.5 ± 0.1 $min^{-1}$, A=0.96, 36-bp substrate; k= 3.4 ± 0.1 $min^{-1}$, A=0.97, 83-bp substrate. In the presence of trap RNA: k = 3.6 ± 0.2 $min^{-1}$, A=0.77, 36-bp substrate; k = 3.6 ± 0.3 $min^{-1}$, A=0.52, 83-bp substrate. Variances are standard deviations from the fit.

**Figure 10**

Estimation of the unwinding step size. Time courses of substrates containing duplex regions of 12 (open squares), 18 (filled squares), 24 (open circles) and 36

(filled circles) bp unwound by NPH-II in the presence of 4mM $CoCl_2$. Substrates contain a 35-U single-strand overhang 3' to the duplex region. Step size and the unwinding (translocation) rate constant were calculated were calculated from at least two independent time courses for each duplex which are overlaid on the plots. Solid lines are best fits to the kinetic model resulting in an unwinding step size of 6 bp and an average unwinding rate constant of $k_g = 13.4 \pm 0.8$ $min^{-1}$.

**Figure 11**

Probing helicase directionality with multipiece substrates (MPS) **a**, Design of the MPS **b**. Unwinding of MPS in 4mM $MgCl_2$ and trap RNA. Unwinding rate constants were similar for all pieces ($k=3.3 \pm 0.5$ $min^{-1}$); reaction amplitudes (A) were MPS 36/75, T36 A=0.74; T75, A = 0.32; MPS 83/28, T83, A=0.43; T28, A=0.27. **c**. Unwinding of multipiece substrates in 4 mM $CoCl_2$ and trap RNA. Kinetic data were analysed as described in Fig. 2, which resulted in average values of $k_g = 12.4 \pm 2.1$ $min^{-1}$ and a step size of 6pb, consistent with the values obtained for oligomers shown in Fig. 2.

**Figure 12**

Processivity of NPH-II **a**, ATP dependence of processivity in 4 mM $MgCl_2$ (filled circles) and 4mM CoCl (open circles). The solid line is a hyperbolic fit: $P = P[ATP]/(Z + [ATP])$, where $P_\infty = k_{U[S]}/(k_{U[S]} + k_\delta)$ reflects the processivity at ATP saturation; $Z$ is the ATP concentration where $P = P_\infty/2$. In 4mM $CoCl_2$, $P_\infty = 1.00 \pm 0.03$ and $Z = 0.50 \pm 0.06$ mM. In 4mM $MgCl_2$, $P_\infty = 0.99 \pm 0.01$ and $Z = 0.14 \pm 0.01$ mM. Processivities were determined from the reaction amplitudes of four duplexes

(12, 18, 24 and 36 bp, Fig. 2) at the ATP concentrations indicated. Amplitudes were obtained from at least three independent experiments. Processivity was calculated by fitting plots of amplitude at constant ATP concentration versus duplex length to Equation 2 using a step size of m=6 (Fig. 2). **b,c,** Dependence of reaction amplitude on ATP concentration for substrates with duplex regions of 12 (filled circles), 18 (open circles), 24 (filled squares) and 36 (open squares) basepairs in 4 mM $MgCl_2$ **(b)** and 4mM $CoCl_2$ **(c)**. Each reaction amplitude was determined in triplicate and the deviation from these independent measurements is indicated by the error bars. The solid lines are fits to equation 1, where $k'_d$ was assumed to equal $K_m$ from multiple turnover ATPase measurements (1.1 mM in $Mg^{2+}$ and 3.5 mM in $Co^{2+}$ (Shuman, 1993; Gross and Shuman 1996), the step size was 6bp (Fig. 2), and $k_p/k_{U[S]}$ was allowed to flout. In both $Mg^{2+}$ and $Co^{2+}$ $k_p/k_{U[S]} = 0.12$.

**Figure 13**

The kinetic scheme for RNA helicase activity by NPH-II. Unwinding initiation and two unwinding/translocation steps are depicted. $ES_1$ and $ES_2$ represent the enzyme substrate complex in non-ATP-bound states, while [$ES_1$-ATP] and [$ES_2$-ATP] represent ATP-bound states. Note that 'ATP-bound' indicates that ATP is bound but not hydrolysed, whereas 'non-ATP-bound' indicates that no nucleotide is bound or that ADP and/or inorganic phosphate are bound. The equilibrium between ATP-bound and non-ATP-bound states is fast compared with translocation with the unwinding rate constant $k_{U[S]}$. $k_p$ (Shuman, 1993; Gross and Shuman, 1996) is the rate constant for enzyme dissociation from subtrate in the ATP-free state, dissociation in the ATP-bound state is

not significant (Fig. 4a) $k_1$ is the rate constant for the unwinding initiation step. Reactions were conducted in the presence of trap-RNA (Fig. 1), thus ES dissociation is irreversible.

5

## Detailed Description of the Invention

The present invention provides an a method for detecting the release of a single-stranded RNA from an RNA duplex which comprises (a) admixing an RNA helicase with the RNA duplex under conditions permitting the RNA helicase to unwind the RNA duplex and release single-stranded RNA, wherein the RNA duplex comprises a first RNA having a first label attached thereto and a second RNA, such first label being capable of producing a luminescent energy pattern when the first RNA is present in the RNA duplex which differs from the luminescent energy pattern produced when the first RNA is not present in the RNA duplex, (b) subjecting the admixture to conditions which permit (i) the RNA helicase to unwind the RNA duplex and release single-stranded RNA, and (ii) the first label to produce luminescent energy, and (c) detecting a change in the luminescent energy pattern produced by the first label so as to thereby detect release of single-stranded RNA from the RNA duplex.

In accordance with the present invention conditions which permit the RNA helicase to unwind the RNA duplex and release single-stranded RNA preferably include, but are not limited to the presence of ATP and a divalent cation, which preferably may be $Mg^{2+}$, $Mn^{2+}$ or $Co^{2}$.

The foregoing method may be carried out in numerous ways which will be readily understood by those skilled in the art. In a presently preferred embodiment of the invention the method utilizes a second label attached to the second RNA such that the luminescent energy produced by the first label interacts with the second label to produce a characteristic pattern when the first and second RNA are present in an RNA duplex, but interacts

differently or not at all when the RNA duplex unwinds. In one embodiment of the invention the first label is covalently attached at the 5' end of the first RNA and the second label, if any, is attached at the 3' end of the second RNA.

In accordance with the foregoing, embodiment the first and second label may comprise different fluorophors having the characteristic that the second label absorbs luminescent energy released from the first fluorophor when it is induced to emit luminescent energy by exposure to a particular type of radiation such as ultraviolet light of a defined wavelength. In one embodiment the first label is fluorescein isothiocyanate and the second label is rhodamine isothiocyanate.

As used herein luminescent energy includes but is not limited to fluorescence, phosphorescence, and chemiluminescence.

In the practice of the methods of the invention the compound capable of inhibiting unwinding activity of an RNA helicase may be a chemically synthesized substrate that preferentially binds over a endogenous substrate to the RNA helicase. In one embodiment of the invention the compound inhibits the accessibility of the ATP to the binding site on the protein thereby enabling the helicase to dissociate from the RNA at appropriate times. In another embodiment of the invention the compound induces a rate-limiting step by blocking and deblocking initiation of the RNA unwinding by the RNA helicase.

In the practice of the methods of the invention the compound capable of inhibiting the unwinding activity of an RNA helicase is present at a concentration capable of

inhibiting the unwinding activity of an RNA helicase. Accordingly, the effective amount will vary with the helicase used.

This invention also provides a method of measuring the rate of release of a single-stranded RNA from an RNA duplex which comprises detecting whether the single-stranded RNA is released from the RNA duplex at predetermined time intervals according to the method and determining therefrom the rate of release of the single-stranded RNA from the RNA duplex.

Furthermore, this invention provides a method of determining whether a compound is capable of modulating the release of a single-stranded RNA from an RNA duplex by an RNA helicase which comprises detecting the release of the single-stranded RNA from the RNA duplex according to the method wherein the compound is added to the mixture of RNA duplex and RNA helicase

Still further, this invention also provides effective amounts of compounds capable of inhibiting unwinding activity of an RNA helicase together with suitable diluents, preservatives, solubilizers, emulsifiers, adjuvants and/or carriers useful in treatment of viral RNA helicase or a viral Hepatitis C. Such compositions are liquids or lyophilized or otherwise dried formulations and include diluents of various buffer content (e.g., Tris-HCl., acetate, phosphate), pH and ionic strength, additives such as albumin or gelatin to prevent absorption to surfaces, detergents (e.g., Tween 20, Tween 80, Pluronic F68, bile acid salts), solubilizing agents (e.g., glycerol, polyethylene glycerol), anti-oxidants (e.g., ascorbic acid, sodium metabisulfite), preservatives (e.g., Thimerosal, benzyl

alcohol, parabens), bulking substances or tonicity
modifiers (e.g., lactose, mannitol), covalent attachment
of polymers such as polyethylene glycol to the compound,
complexation with metal ions, or incorporation of the
compound into or onto particulate preparations of
polymeric compounds such as polylactic acid, polglycolic
acid, hydrogels, etc, or onto liposomes, micro emulsions,
micelles, unilamellar or multi lamellar vesicles,
erythrocyte ghosts, or spheroplasts. Such compositions
will influence the physical state, solubility, stability,
rate of *in vivo* release, and rate of *in vivo* clearance of
the compound. The choice of compound will depend on the
physical and chemical properties of the compound capable
of alleviating the symptoms of a viral RNA infection.

This invention is illustrated in the Experimental Details
section which follows. These sections are set forth to
aid in an understanding of the invention but are not
intended to, and should not be construed to, limit in any
way the invention as set forth in the claims which follow
thereafter.

## Experimental Details

The DExH helicase NPH-II from vaccinia virus (Shuman,
1992) was subjected to quantitative kinetic analysis that
varied in composition and length. Kinetics of unwinding
were monitored using gel-shift electrophoresis and
fluorescence energy transfer methodologies. The RNA
substrates contained a single-strand 3' overhang, which
is required for NPH-II unwinding activity (Shuman, 1993).
The single-strand 3' overhang was identical in length and
sequence for every substrate (Fig. 9). Unwinding
reactions were preformed under single-turn-over
conditions with respect to the RNA substrate. A large

excess of nonspecific trap RNA (de la Cruz, 1999) was added to prevent helicase from reassociating with duplex once it falls off during the course of reaction.

In the absence of trap RNA, the unwinding rate and reaction amplitude (defined as the final fraction of unwound RNA) were both insensitive to duplex length (Fig. 9). Each reaction was first-order with a rate constant of $3.5 \pm 0.2$ min$^{-1}$ (Fig. 9). In the presence of trap RNA, the rates remained independent of duplex length however, the reaction amplitude decreased with increasing duplex length (Fig. 9). These observations provide three mechanistic insights. First, the fact that long duplexes can be unwound at all in the presence of trap RNA provides strong qualitative evidence that the helicase is a processive enzyme consistent with previous multiple-turnover studies. Second, the dependence of amplitude on duplex length indicates that more protein dissociates from an RNA substrate when the duplex is longer indicating that more protein dissociates from an RNA substrate when the duplex is longer, indicating that more unwinding steps may be required for a long duplex, and there is a specific degree of processivity for the NPH-II enzyme (Fig. 9). Last, the similar rates observed for the unwinding of different duplex lengths indicate that individual unwinding steps do not limit the reaction rate under these conditions. Rate-limiting events during translocation would result in a length-dependent lag phase in each time course.

To evaluate helicase step size and to provide an additional proof of processivity, it was necessary to monitor individual unwinding steps. Conditions were sought under which helicase translocation becomes rate limiting. Variation in temperature and pH did not cause

the rates to become increasingly sensitive to duplex length (E. Jankwsky et al., unpublished data); however, marked effects were observed when $Mg^{2+}$, which is the cofactor for ATP hydrolysis, was replaced by $Co^{2+}$. The unwinding reactions displayed pronounced lag phases which increased incrementally with the duplex length (Fig. 10). The data were fit numerically to a kinetic model that relates the translocation rate constant to step size and duplex legngth (Material and Methods). From this analysis, the unwinding step size of NPH-II was estimated to be six base pairs (bp) and the unwinding rate constant (for each translocative step in $Co^{2+}$ at an ATP concentration of 3.5 mM), $k_u$, was $13.4 \pm 0.8$ $min^{-1}$. Using the step size of 6 bp, it is possible to calculate a lower limit for the translocation rate constant in $Mg^{2+}$. In these conditions, $k_u$ was greater than 350 $min^{-1}$, indicating that translocation in $Mg^{2+}$ is at least 25-fold faster in $Co^{2+}$. The slower unwinding rate in $Co^{2+}$ is not attributable to inhibition of ATPase activity, as kinetic parameters for hydrolysis of ATP are similar in $Co^{2+}$ and $Mg^{2+}$ (E. Jankowsky et al., unpublished data).

The existence of a defined step size indicates regularity in the translocation process; that is, unwinding is not random with respect to individual translocation rates and the number of bp displaced in one unwinding step. The step size obtained herein corresponds to about half of a helical turn and is very similiar to the unwinding step size of the UvrD DNA helicase of 4 - 5 bp (Ali and Lohmann, 1997). It is important to note that the unwinding step size is an average value that may not necessarily reflect actual microscopic translocation steps of a helicase (Ali and Lohmann, 1997).

Although the above results suggest that RNA unwinding occurs in consecutive steps, the assays that we used are designed to monitor only the very last event in strand displacement (one does not see a signal until the duplex is completely unwound). Therefore, it is impossible to distinguish between directional translocation and translocation that occurs through random facilitated diffusion (Shimamoto, 1999; Kelemen and Raines, 1999). To determine which of these mechanisms applies, detection of an unwinding intermediate was needed. This was accomplished by using multipiece substrates (MPS), consisting of a continuous bottom strand that is annealed to two adjacent pieces of top-strand RNA (Fig. 3a). The top-strand pieces were generated by site-specific cleavage of a single continuous piece of top-strand RNA (Fig. 11a). The top-strand (first RNA molecule) pieces were generated by site-specific cleavage of a single continuous piece of top-strand RNA using synthetic DNAzyme endonucleases (Santoro and Joyce, 1996). The two resultant pieces had different lengths and could therefore be distinguished by their respective electrophoretic mobilities (Fig. 11b, 11c). To prevent the results from being biased by the relative length of the top-strand pieces we designed two different sets of MPS (Fig. 11a). All MBPS unwinding reactions were carried out under single-turnover conditions with respect to the RNA substrate, and in the presence of trap RNA.

NPH-II unwound both sets of MPS (Fig. 11b), indicating that the helicase can proceed through nicks in the top strand of the substrate. In the presence of $Mg^{2+}$, all pieces were displaced with apparent first-order kinetics with similar rate constants, $k = 3.3 \pm 0.5$ $min^{-1}$ (Fig. 11b). For both sets of MPS, the piece that was bound farthest from the overhang was displaced with a lower

amplitude than the piece located closer to the single-strand 3' overhang (Fig. 11b). This implies that fewer unwinding steps were required for the displacement of the piece closer to the overhang. The fact that these effects depend exclusively on the location of the top strands relative to the single-strand 3' overhang (rather than their length) strongly suggests that the strand displacement progresses in a distinct 3'-to-5' direction with respect to the bottom strand.

The similar unwinding rates for both pieces of top-strand RNA indicate that neither a late step in the reaction, such as the final strand separation, nor translocation itself, limits the rate of the overall process in $Mg^{2+}$. A late rate-limiting step would result in a slower rate for unwinding of the piece farthest from the overhang because two strand separations are required for unwinding of the second piece. A rate-limiting translocation would cause a lag phase in the time courses as observed in the presence of $Co^{2+}$ (Fig. 10). Thus in the presence of $Mg^{2+}$, an initiation step at the very begining of the unwinding process limits the rate of the overall reaction.

By contrast, reactions conducted in the presence of $Co^{2+}$ displayed a pronounced lag phase attributable to rate-limiting translocation steps (Fig. 11c). Notably, the displacement of the two pieces occurred with different lag phases. The lag was largest for the piece farthest from the overhang, reflecting an increase in the number of unwinding steps that are required as the helicase moves away from the single-strand 3' overhang. The effects were exclusively dependent on the location of the pieces relative to the over hang and not on their length indicating a distinct 3'-to-5' directionality in the

progression of unwinding with respect to the bottom strand.

Having established that the helicase unwinds RNA substrates in a processive directional fashion with a distinct unwinding step size it was of interest to correlate this process with the role of ATP. The effect of ATP on enzyme processivity (P) was of particular interest (Fig. 12). Processivity reflects the probability that the helicase will perform the next unwinding step rather than dissociate from the substrate (Lohmann and Bjoernson, 1996). Quantitation of processivity was carried out by determining the reaction amplitude in the presence of trap RNA, such that all dissociation of protein from the RNA substrate during unwinding was effectively irreversible. Processivity decreased with decreasing ATP concentration (Fig. 12a), which indicates that the helicase dissociates more readily from RNA in non-ATP-bound states than in the ATP-bound state, consistent with previous studies of RNA binding by NPH-II (Shuman, 1992). In addition, the processivity at ATP saturation approaches $P = 1$, regardless of whether $Co^{2-}$ or $Mg^{2+}$ are the cofactors for ATP hydrolysis (Fig. 12a). This indicates that NPH-II in the ATP-bound state does not significantly dissociate from the RNA substrate, and that dissociation of protein from RNA occurs predominantly in non-ATP-bound states. This is highly instructive because it shows that ATP binding and not just the consumption of ATP through hydrolysis, is of critical importance in the helicase mechanism.

Although RNA unwinding activity by NPH-II is dependent on ATP hydrolysis (Shuman, 1992), one must establish quantitative link between ATP utilization and a specific

amount of unwinding to conclude that DExH/D proteins behave as true molecular motors (Schnapp, 1995). Plots of reaction amplitude versus ATP concentration resulted in sigmoidal curves (Fig. 12b, 12c) that are affected by duplex length: the longer the duplex, the more pronounced the sigmoidal shape of the time course. These results, together with the observation of a discrete step size and the fact that NPH-II does not dissociate in the ATP-bound state are consistent with the kinetic scheme shown in Fig. 13. This scheme was used to derive an explicit equation that describes the plots of reaction amplitudes versus ATP concentration (Fig. 12b, 12c).

$$A = (1 - x) \cdot \left( 1 + \frac{k_c}{k_{U[S]}} \cdot \frac{K'_d}{[ATP]} \right)^{-U_m}$$

The fit of this expression to the data establishes a direct relationship between processivity and ATP concentration, indicating that translocation is coupled to the binding of ATP. This link between ATP utilization and directional movement supports the assertation that NPH-II is a processive molecular motor.

The results suggest the following basic mechanism for RNA duplex unwinding by the DExH RNA helicase NPH-II (Fig. 13); unwinding is preceded by a slow initiation step (2.3 $\pm$ 0.2 in $Co^{2+}$, 3.5 $\pm$ 0.3 in $Mg^{2+}$). Subsequent unwinding occurs in distinct consecutive steps of roughly one-half helix turn in a defined 3'-to-5' direction with respect to the single-strand 3' overhang. The helicase

translocates rapidly along the RNA substrate, unwinding RNA with a rate that is dependent on identity of the metal ion cofactor (13.4 ± 0.8 $min^{-1}$ per step for $Co^{2+}$; ≥ 350 $min^{-1}$ per step for $Mg^{2+}$). During each step, a fraction of protein, predominantly in non-ATP-bound states, dissociates from the RNA. The dependence of reaction on ATP hydrolysis and the direct connection between ATP binding and translocation indicate that NPH-II is a processive directional motor for unwinding RNA. This activity DexH/D proteins might ensure processive, regulated rearrangement of structured RNA in macromolecular assemblies during processes such as RNA splicing, export or translation initiation. A rate-limiting step before translocation would provide a straight-forward way to control unwinding by blocking and deblocking an early initiation event. Alternatively, factors that control the local concentration of ATP or accessiblity of the ATP binding site on the protein could regulate processivity, enabling the helicase to dissociate from RNA at appropriate times.

DExH/DEAD box proteins (putative RNA helicases) are important in all aspects of RNA transcription, maturation and translation. A step towards understanding the function(s) of this class of enzymes at the molecular level is to investigate the mechanism underlying duplex RNA unwinding by the vaccinia virus DExH RNA helicase NPH-II.

Transient kinetic experiments were performed using a series of fluorescent dye labeled RNA substrates with duplex regions of different length. The unwinding reaction was monitored continuously in real time by measuring the changes in fluorescence energy transfer upon the unwinding reaction.

Timecourses under single turnover conditions displayed significant dependence on the length of the duplex region in terms of reaction rate and reaction amplitude. Reaction rates were also affected by the nature of the divalent cation cofactor. In the presence of $Co^{2+}$ timecourses were found to have a significant lag phase, increasing with the duplex length. In the presence of $Mg^{2+}$ no comparable lag phase was observed, but reaction rate as well as reaction amplitude were greater as compared to the reactions with $Co^{2+}$. Dependent on the duplex length, the ATP concentration affected the reaction rate and amplitude with both metal cofactors.

These findings suggest a basic mechanism for the translocation/unwinding reaction consisting of consecutive events of ATP binding and translocation. Quantitative description of this mechanism leading to the rate and step size for the translocation/unwinding reaction follows.

*Design of the RNA substrates*. These studies used the RNA helicase, vaccinia virus DExH protein NPH-II. The protein was expressed in baculavirus infected insect cells (Gross and Shuman, 1995). The NPH-II helicase requires the substrate to have single stranded overhangs 3'-end to the duplex region (Shuman, 1992), which are necessary for the helicase to bind the substrate (Shuman, 1993). In order to prevent binding of the protein at multiple sites, a substrate for mechanistical studies should contain solely one single stranded region. This single stranded region should be constant for a series of substrates where the length of the duplex region is variable.

Two different ways to design the substrates: by chemical synthesis with subsequent template directed ligation (Moore and Sharp, 1992) and by *in vitro* transcription from PCR generated templates (Chabot, 1992) with subsequent DNAzyme processing (Santoro and Joyce, 1997) in order to produce perfect blunt ended duplexes. Chemical synthesis bears the advantage of complete flexibility in the sequence choice and allows the incorporation of a variety of modifications including nucleoside and backbone modifications as well as fluorescent labels. The method is limited in terms of the length of the oligos which can be produced. *In vitro* transcription from PCR generated templates does not have these limitations for the length of the oligos but this method is not completely variable concerning the sequence and it does not allow the incorporation of extensive modifications.

Exploiting the respective advantages of both methods we designed two series of substrates. The series based on chemical synthesis contains a U-35 single stranded overhang and duplex regions from 12 to 36 basepairs (Fig. 2). The series based on *in vitro* transcription contains a 33 mucleotide overhang and duplex regions from 36 83 basepairs. The unwinding reaction of the substrates was monitored by separation of unwound strands from intact substrate on native gel electrophoresis. All substrates tested were unwound by NPH-II (Fig. 2).

*Effect of trap* RNA *on the unwinding reaction.* Excess single stranded RNA (Trap RNA) is required for single turnover reactions where dissociation of protein from the substrate has to be irreversible, i.e. trap RNA has to prevent re-binding of protein to the substrate during the

reaction (Fig. 3a). The effect of trap RNA addition with two substrates was tested: one with a 36bp duplex region and one with a 83bp duplex region. Reaction rates and amplitudes without trap addition were comparable with both substrates (Fig. 3b). The addition of trap RNA did not significantly change the reaction rates with both substrates. However, reaction amplitudes decreased with both of the substrates as compared to the reactions without trap (Fig. 3b), whereby the reaction amplitude with the longer substrate (LS83) was lower than the amplitude with the shorter substrate (LS36). Thus, the duplex length does not affect the rate of unwinding suggesting that the rate-limiting step for the overall reaction is an event which is not a potential translocation. However, the different reaction amplitudes indicate that protein dissociates off the substrate more frequently during the of unwinding of longer duplexes, suggesting that the number of dissociation "events" increases with increasing duplex length. This is an indirect indication that there are distinct consecutive steps in the unwinding reaction, even if this is not reflected in the reaction rate (Fig. 1).

*Monitoring duplex unwinding by fluorescence measurements.* In order to obtain data of higher time resolution, the unwinding reaction was monitored by measuring changes in fluorescence in real time upon the unwinding of fluorescently labeled duplexes (Fig. 4a). Since the data obtained by gel shift and by fluorescence are superimposable, the real time fluorescence method provided also the control that no artifacts were introduced by the gel separation method (Fig4b). The reaction rates with both substrates tested (18bp duplex

and 36bp duplex) were similar (Fig.4b). The reaction
amplitude of the 36bp duplex was lower than that of the
18bp duplex. Thus, these observations agree with the
data described above (Fig. 3)

*Effect of the ATP concentration on the unwinding
reaction.* The decreasing reaction amplitude with
increasing duplex length in reactions where protein
dissociation from the substrate was irreversible (Figs.
3 and 4) indicates that with each "unwinding step" a
certain fraction of protein dissociates from the
substrate (Fig. 1). For the understanding of the
mechanism of unwinding it is of importance to know
whether this dissociation occurs in an ATP-bound state of
the protein or in a non-ATP-bound state or in both
states. Experimentally, this question can be accessed by
measuring the effect of ATP concentration variation on
the reaction amplitude. Decreasing reaction amplitudes
with decreasing ATP concentrations would indicate that
dissociation occurs in a non-ATP-bound state.
Dissociation in an ATP-bound state would be indicated by
differences in the reaction amplitudes with duplexes of
different length under ATP saturation of the system.
Measurements conducted of the reaction amplitude in
dependence on the ATP concentration with a 36bp substrate
and a 83bp substrate (Fig. 5). The reaction amplitude
decreased with decreasing ATP concentrations, indicating
clearly that dissociation occurs at non-ATP bound states
of the protein. The differences in the reaction
amplitude of both substrates near ATP saturation suggest
further that the protein dissociates also in the ATP-
bound state. (Fig. 5).

*Effect of Mg²⁺ substitution on the unwinding reaction.*
At the reaction conditions tested so far, the only
response to the variation in the duplex length was the
reaction amplitude. Although this suggests a processive
unwinding reaction, the fact that no effect was found on
the rates of the unwinding reaction indicates that not a
potential translocation limits the overall rate of the
reaction. However, for the quantification of the
unwinding steps in terms of the step size and individual
rate constants it is necessary that the translocation
directly affects the reaction rate. Therefore, attempts
were made to decrease the rate of translocation relative
to the rate limiting step such that intermediates of the
unwinding reaction would be kinetically detectable and
translocation would be directly reflected in the
unwinding timecourse (Fig. 1). Variation in pH and
temperature did not result in the desired changes in the
timecourses (not shown). Subsequently, we examined
whether a substitution of Mg²⁺ with other divalent
cations, which act as cofactor for the ATP hydrolysis,
provides reaction conditions where the translocation
would be slower relative to the previously rate limiting
step. Recently, only Mn²⁺ and Co²⁺ were found to
substitute for Mg²⁺ in the unwinding reaction for NPH-II
(Shuman, 1992). In reactions with RNA-protein pre-
annealing and in the presence of trap RNA, Mn²⁺ did not
change the timecourses as compared to the reactions with
Mg²⁺ (Fig. 6). However, substituting Mg²⁺ with Co²⁺
resulted in a substantial change in the observed
timecourse (Fig. 6). With Co²⁺, the timecourse displayed
a pronounced lag phase, suggesting reaction intermediates
(Fig. 1). This assumption was supported by measuring
reactions with substrates with duplex regions of
different length in the presence of Co²⁺. The timecourses

showed an increasing lag phase with increasing duplex
length, i.e. the longer the duplex, the more
intermediates appear in the unwinding reaction (Fig. 7).
This indicated that in the presence of $Co^{2+}$, it can be
directly observed that the reaction proceeds in distinct
consecutive steps and can therefore be considered to be
processive. In accordance with the results described
above (Fig. 2 and 3), the reaction amplitude decreased
with increasing duplex length (Fig. 7), indicating that
protein dissociates more frequently during the unwinding
of longer duplexes.

*Employing multi-piece substrates for probing the
directionality of the unwinding reaction.* The results
described above (Figs. 2-7) suggested that the unwinding
of RNA duplexes by NPH-II is in fact processive. The
second basic feature of the unwinding reaction, the
directionality of the process, could not be accessed yet.
Since monitoring the unwinding reaction with the
described methods bears the disadvantage that the
observed unwinding is caused by an event at the end of
the unwinding reaction (Fig. 1), no direct evidence for
directionality can be provided. Although a processive
unwinding together with the binding of the protein at the
single stranded overhang of the substrate indirectly
argues for a certain directionality of the process, a
number of alternative unwinding mechanisms (for instance
looping of the single-stranded-bound protein into the
duplex region) cannot be ruled out. In order to prove
directionality unambiguously, we attempted to employ a
more direct assay, where, beside, the unwinding of the
"whole" duplex at least one intermediate has to be
monitored during the reaction. We accomplished that by
designing multi-piece-substrates (MPS), which comprise a

regular bottom strand but two adjacent to each other binding top strand pieces (Fig. 8a). Provided that the two pieces can be separated from each other on native PAGE, it should be possible to observe the separate displacement of the two pieces as the helicase translocates in a directional way. In order to exclude effects of the length of the different pieces *per se*, we designed two MPS; one with the longer piece next to the single stranded overhang, and another one with the shorter piece next to the single stranded overhang (Fig. 8a). The unwinding reactions were performed with protein-RNA pre-annealing and in the presence of trap RNA, such that dissociation of protein from the substrate was irreversible.

Both MPS were unwound by NPH-II, emphasizing that the helicase tolerates nicks in the top strand of the substrate. In the presence of $Mg^{2+}$, both pieces were displaced with a similar rate (Fig. 8b). The piece binding more distal to the overhang was displaced with a lower amplitude as compared to the piece binding closer to the single stranded overhang. This was observed for both MPS, and, therefore, the amplitude effects are caused only by the position of the pieces relative to the overhang. These results support the findings with the regular substrates (Figs. 2,3), where, although more protein dissociates from the substrate with increasing duplex length, the reaction rate is not limited by the translocation. Moreover, the fact that the amplitude was lower for the piece more distal to the overhang but the reaction rates of both pieces were similar suggests that the event which limits the rate of the overall reaction is before the translocation process, i.e. the unwinding

initiation is likely to limit the overall reaction in the presence of $Mg^{2+}$.

In the presence of $Co^{2+}$, the displacement of both pieces occurred with different lag phases (Fig. 8c). The lag for the pieces next to the overhang was always smaller, than the lag for the pieces more distal to the overhang (Fig. 8c), indicating that one piece is displaced after the other and that this displacement process has a directionality: initiating from the single stranded region the helicase translocates towards the other end of the duplex while it unwinds it. Moreover, the reaction amplitude for the piece more distal to the overhang was smaller then the amplitude for the piece next to the overhang, indicating that also in the presence of $Co^{2+}$ protein dissociates from the substrate more frequently with increasing duplex length.

**Materials and Methods**

NPH-II was expressed and purified as described (Gross and Shuman, 1995). RNAs were prepared by *in vitro* transcription of PCR-generated T7 transcription templates (Jankowsky and Schwenzer, 1996) or by chemical synthesis (Wincott et al., 1995). The PCR-amplified DNA templates represent a segment of the ampicillin-resistance gene of the pBS(+/-) phagemid (Stratagene). To generate perfect blunt-end duplexes, the RNA pieces were trimmed by site-directed processing using engineered DNAzymes (Santoro and Joyce, 1997; Pyle et al., 2000) with 12 nucleotides on each of the binding arms. Bottom-strand RNAs were joined from two separately synthesized oligonucleotides by template-directed ligation using T4 DNA ligase (Moore and Sharp, 1992) RNA duplexes were formed by combining the botton-strand RNA with a five-fold molar excess of $\gamma^{32}$

P-labelled top strand in 10mM MOPS, 6.5, 1mM EDTA. The
solution was heated to 95°C for 2 min and cooled to room
temperature over 90 min. Duplexes were separated from
single-strand RNA by native PAGE, visualized by
5      radiolytic scanning (Packard Instant Imager) and excised
from the gel.

**Unwinding reactions**

Unwinding reactions were performed at room temperature in
10     $30\mu l$ of 40mM Tris-HCl buffer, pH 8.0 and 4mM $MgCl_2$ or
$CoCl_2$. The reaction also contained 25mM NaCl, which was
introduced with the protein storage buffer. In a typical
reaction, 1-2nM RNA substrate was incubated with 10-15nM
NPH-II in reaction buffer without ATP at room temperature
15     for 5-7 min. Longer pre-incubation time did not change
the reaction kinetics. Saturation of substrate with
protein before the reaction was verified by gel-shift
analysis (Lohmann and Bjoernson, 1996). The unwinding
reaction initiated by adding the ATP to a final
20     concentration of 3.5mM unless otherwise stated. Aliquots
at the respective time points were quenched with two
volumes of stop buffer 25 mM EDTA, 0.4% SDS, 0.05% BPB,
0.05% XCB, 10% glycerol containing 200nM of unlabelled
top-strand RNA to prevent re-annealing of unwound
25     duplexes during electrophoresis. Reannealing of unwound
duplexes during the reaction did not affect unwinding
kinetics under any reaction conditions as verified by
independent measurements of association rate constants of
the substrate strands. Excess RNA (Trap RNA) (200 nM
30     final concentration added with the ATP) was a single-
strand of 39-nucleotides of unrelated sequence. Higher
concentrations of trap RNA did not change observed
reaction amplitudes.

Unwinding reactions were also monitored in real time using fluorescence energy transfer experiments on substrates labelled at the 3' and 5' ends of the duplex terminus farthest from the single stranded 3' overhang. These measurements were superimposable with results from gel-shift measurements and confirmed the first-order nature of the time courses as well as the rate constants.

## Kinetic analysis

Data were fit numerically using the FITSIM software package (Barshop and Frieden, 1983). Time courses were corrected for the reaction amplitudes, and initial kinetic parameters were determined using the KINSIM software (Barshop and Frieden, 1983). Unwinding step size and rate constants were determined from time courses in $Co^{2+}$ using a kinetic model in which the unwinding reaction consists of N consecutive first-order reactions where N is the number of kinetic steps. Rate constants (except for the first step see below) were linked, that is, forced to yield the same value in the fitting. The linked rate constants and the first rate constant were allowed to float simultaneously. On the basis of the observation than an initial step is slower than subsequent steps in $Mg^{2+}$ (see Fig. 11b and text), the first kinetic step was defined as having a different rate constant ($k_1$) than subsequent kinetic steps ($k_u$). Using this model, increasing numbers of steps (N) were examined iteratively for each duplex until $k_1$ and $k_u$ approached constant values for the different duplexes. Convergence occurred when $k_1 = 2.3 \pm 0.2$ $min^{-1}$ and $k_u = 13.4 \pm 0.8$ $min^{-1}$.

Note that $k_u$ is an apparent rate constant that depends on the ATP concentration according to $k_u = k_{u[S]}$ [ATP/(ATP + $K'_d$), where $k_{u[S]}$ is the respective rate constant at ATP

saturation. The step size (m) was calculated according to m=L(N-y), where y is the number of kinetic steps do not contribute to the actual strand displacement and L is the duplex length. A step size of m=6 and a value of y=1 were consistently calculated for all duplexes λ including multi-piece substrates.

The lower limit for the translocation rate constant in $Mg^{2-}$ was estimated by considering that a lag phase was not observed with the longest (83 bp) duplex (Fig. 9b). Assuming an unwinding step size identical to that in $Co^{--}$ (6 bp), and that $k_u$ must be equal or greater than a value that does not cause an apparent lag phase in 14 unwinding steps, the translocation rate constant was estimated as $k_u > \sim 350$ $min^{-1}$.

Equation (1) was derived from the expression describing the dependence of reaction amplitude (A) on the processivity (P):

$$A = (1 - x) P^{j/m}$$

where $\chi$ is the fraction of protein that dissociates from the substrate before unwinding occurs. $P$ is then substituted with a term that relates processivity and ATP concentration under the conditions specified by the scheme in Fig. 13.

$$P = \dfrac{k_{max}\left(\dfrac{|ATP|}{K_d' + |ATP|}\right)}{k_{max}\left(\dfrac{[ATP]}{K_d' + [ATP]}\right) + k_f\left(1 - \dfrac{[ATP]}{K_d' + [ATP]}\right)}$$

where $K_d'$ is the apparent dissociation constant of ATP from the enzyme substrate complex.

**RNA Substrate Preparation**

*Chemical Synthesis:* RNA oligonucleotides were prepared by chemical synthesis using phosphoramidite chemistry (amidites purchased from Glen Research) on an ABI 392 RNA/DNA synthesizer. Deprotection of the crude oligonucleotides was carried out according to standard protocols (Wincott et al., 1995). All RNA oligonucleotides were purified on denaturing PAGE.

The bottom strand RNAs were joined out of two separately synthesized oligonucleotides by template directed ligation using T4 DNA ligase (Moore and Sharp, 1992). The ligated products were purified on denaturing PAGE.

*Fluorescent Labeling:* Amino linkers were placed in the 3' or 5' position of the respective RNA during the synthesis. After removal of all deprotection groups, the modified RNA was labeled with fluorescein-or rhodamine-isothiocyanate (Sigma), respectively. Labeling reactions were carried out in the dark for 12-18 hours with 50 mM

dye-isothiocyanate and RNA concentrations below 50 $\mu$M in 0.1 M sodiumbicarbonate (pH 9.0) and 20% (v/v) DMSO for the fluorescein-isothiocyanate labeling and 50% (v/v) DMSO for the rhodamine-isothiocyanate labeling. The excess rhodamine-isothiocyanate was removed by repeated phenol extractions followed by ethanol precipitation. The excess fluorescein-isothiocyanate was removed by repeated ethanol precipitations. All labeled RNAs were finally purified on denaturing PAGE.

*In vitro transcription:* RNAs for the multi-piece-substrates were prepared by *in vitro* transcription of PCR generated templates (Chabot, 1992). The PCR-amplified DNA-templates represent a segment of the ampicillin resistance gene of the pBS (+/-) phageimid (Stratagene). Templates for bottom and top strand RNAs were separately amplified from ScaI linearized phageimid using different pairs of primers with the respective sense primer containing the binding sequence as well as the T7 promoter sequence. 100$\mu$L PCR reactions were carried out for 30 cycles (52$^0$C, 72$^0$C, 94$^0$C, 1 min each) followed by a 7 min final extension at 72$^0$C. Homogeneity of the PCR products was verified on a 2% agarose gel. The PCR reaction solutions were extracted with an equal volume of phenol, followed by extraction with chloroform isoamylalcohol (Sambrook et al., 1989). Not incorporated dNTPs were removed by SEC (NAP-5, Pharmacia). Subsequently, the volume of the solution was reduced in a Speedvac concentrator (Savant). The obtained DNA templates were used for *in vitro* transcriptions with T7 polymerase according to standard procedures. The transcribed RNAs were purified on denaturing PAGE.

The top strands for the Multi-Piece-Substrates were produced by site directed processing using an engineered DNAzyme (Santoro and Joyce, 1997). DNAzymes with 12 nucleotides in each of the binding arms were designed to cut at the desired positions. The DNAzyme reactions (10$\mu$M RNA, 30$\mu$M DNAzyme) were carried out for 4h at 40$^{\circ}$C followed by ethanol precipitation. Subsequently, the DNAzyme was destroyed by RQ RNAse free DNAse (Promega) in a 100$\mu$L volume with 15units DNAse for 60 min at 37$^{\circ}$C. The RNA was ethanol precipitated and the products were purified by denaturing PAGE.

Duplexes were formed by combining the bottom strand RNA with a 5 fold molar excess of labeled (either radioactively or fluorescently) top strand in 10mM MOPS (pH 6.5), 1mM EDTA. The solution was heated to 95$^{\circ}$C and cooled to room temperature within 90 min. Duplexes were separated from single stranded RNA on native PAGE. The RNA was visualized either by UV-shadowing or by radiolytic scanning (Packard Instant Imager), cut out, eluted, and ethanol precipitated.

**Helicase reactions**

Unwinding reactions were carried out at room temperature in 40 mM Tris/HCl (pH 8.0) and 3mM MgCl$_2$ (MnCl$_2$, CoCl$_2$), 20mM NaCl was present in the reaction due to introduction with the protein storage buffer. In a typical reaction, 3nM RNA substrate was incubated with 10-15 nM NPH-II in reaction buffer without ATP at room temperature for 7 min. Longer incubation time did not change the observed reaction kinetics. The reaction was started by adding the ATP. In reactions with trap RNA, the trap was added together with the ATP at the reaction start.

*Gel shift measurements:* For the reactions monitored by gel shift PAGE, reactions were performed in a volume of 30 $\mu$L. Aliquotes were taken at appropriate times and combined with two volume of stop buffer (25mM EDTA, 0.4% SDS, 0.05% BPB, 0.05% XCB, 10% glycerol), containing 200nM of unlabeled top strand in order to prevent re-annealing of unwound duplexes during electrophoresis. Unwound strands were separated from intact substrate on native PAGE and the amount of unwound duplex was determined using a Molecular Dynamics PhosphorImager and the Imagequant Software.

*Fluorescence Measurements:* For the reactions monitored by fluorescence measurements, reactions were performed in fluorescence cuvette (600 $\mu$L) in an Aminco SLM AB2 fluorescence spectrometer. Excitation wavelength was set at 492 nm, (8nm slid width) emission was recorded at 518 nm (8 nm slid width, PMT sensitivity 600-800V). The reaction was started as described and measurements were taken automatically in fixed intervals.

Employing a series of designed model substrates, it was shown thar the unwinding of RNA duplexes by the DExH protein NPH-II is processive. In the presence of $Mg^{2+}$ the translocation does not limit the overall reaction rate. The rate-limiting step of the unwinding reaction is likely to be the unwinding initiation. The sensitivity of the reaction amplitude to the duplex length indicates that during each "unwinding step" a certain fraction protein dissociates from the substrate. The dependence of the reaction amplitude on the ATP concentration emphasizes that this dissociation occurs in non-ATP bound states of the protein as well as in ATP-bound states of the protein.

Also developed was an assay to test the directionality of the unwinding process and showed that the unwinding process has a defined directionality: initiating from the single stranded region the helicase translocates towards the other end of the duplex while it unwinds it. The proof of the processivity and directionality of the unwinding process is the prerequisite for quantitative characterization of the helicase reaction which is necessary to derive functional models.

## References

Ali, J.A., and Lohmann, T.M. (1997) "Kinetic Measurement of the Step Size DNA Unwinding by *Escherischia coli* UvrD Helicase", Science, 275, 377-380.

Barshop, B. A. and Frieden, C. (1983) "Analysis of Numerical Methods For Computer Simulation of Kinetic Processes: Development of KINSIM--A Flexible Portable System. Anal. Biochem. 130, 134-145.

Chabot, B. (1992) "Synthesis and Purification of RNA Substrates, in RNA Processing: A Practical Approach", Higgins, S.J. and Hames, B.D. Eds., IRL Press, Oxford, U.K., pp 1-31.

de la Cruz, I., Kresler, D. and Linder P. (1999) "Unwinding RNA in Saccharomyces Cerevisiae: DEAD-Box Proteins and Related Families," Trends Biochem. Sc. 24, 192-198.

Gross, C.H. and Shuman, S. (1995) "Mutational Analysis of Vaccinia Virus Nucleoside Triphosphate Hydrolase II, a DExH Box RNA Helicase", J. Virol., 69, 4727-4736.

Gross, C.H. and Shuman, S. (1996) "Vaccinia Virus RNA Helicase: Nucleic Acid Specificity in Duplex Unwinding, J. Virol, 70, 2615-2619.

Jankowsky, E. and Schwenzer, B. (1996) "Efficient Improvement of Hammerhead Ribozyme Mediated Cleavage of Long Substrates by Oligonucleotide Facilitators" Biochemistry 37, 15313-15321.

Jeltsch, A. and Pingoud, A. (1998) "Kinetic Characterization of Linear Diffusion of the Restriction Endonuclease EcoRV on DNA, Biochemistry 24, 2160-2169.

Kadare, G. and Haenni, A. L., (1997) "Virus encoded RNA Helicases," J. Virol 71, 2583-2590.

Kelemen, B. R. and Raines, R. T. (1999) "Extending the Limits to Enzymatic Catalysis: Diffusion of Ribonuclease A in One Dimension" Biochemistry 27, 5302-5307.

Lohmann, T. M. and Bjoernson, K.P. (1996) "Mechanism of Helicase Catalyzed DNA Unwinding", Annu. Rev. Biochem. 65, 169-214.

Moore, M.J. and Sharp, P.A. (1992) "Site Specific Modification of Pre-Messenger RNA-the 2'-Hydroxyl Groups at the Splice Sites", Science, 256, 992-997.

Pyle, A. M., et al., (2000) "Using DNAzymes to Cut, Process and Map RNA Molecules For Structural Studies or Modification" Methods Enzymol 317, 140-146.

Santoro, S.W. and Joyce, G.F. (1997) "a General Purpose RNA-Cleaving DNA Enzyme", Proc. Natl. Acad. Sci., USA, 94, 4262-4266.

Schnapp, B. Molecular Motors, (1995) "Two Heads Are Better Than one" Nature 373, 655-666.

Shimamoto, N. (1999) "One-Dimensional Diffusion of Proteins Along DNA, J. Biol. Chem. 274, 15239-15296.

Shuman, S. (1992) "Vaccinia Virus RNA Helicase: An Essential Enzyme Related to the DE-H Family of RNA Dependent NTPases", Proc. Natl. Acad. Sci. USA, 89, 10935-10939.

Shuman, S. (1993) "Vaccinia Virus RNA Helicase, J. Biol. Chem., 268, 11798-11802.

Staley, J. P. and Guthrie, C. (1998) "Mechanical Devices of the Spliceosome: Motors Clocks Springs and Things" Cell 90, 1041-1050.

Wagner, I.D.O., et al., (1998) "The DEAH-Box Protein Prp 22 is an ATPase that Mediates ATP Dependant mRNA Release From the Spliceosome and Unwinds RNA Duplexes," EMBO J. 17, 2926-2937.

Wincott et al. (1995) "Synthesis, Deprotection, Analysis and Purification of RNA and Ribozymes", Nucleic Acids Res., 23, 2677-2684.

Xiang, Q., et al., (1998) "Sequence Specificity of a Group II Intron Ribozyme: Multiple Mechanisms For Promoting Unusually High Discrimination Against Mismatched Targets" Biochemistry 37, 3839-3849.

Zimmeric, C. and Frieden, C. (1998) "Analysis of Progress Curves by Simulations Generated by Numerical Integration" Biochem. I. 258, 381-387.

44

What is claimed:

4.  A method for detecting the release of a single-
    stranded RNA from an RNA duplex which comprises:

    a)  admixing an RNA helicase with the RNA duplex
        under conditions permitting the RNA helicase
        to unwind the RNA duplex and release single-
        stranded RNA, wherein the RNA duplex comprises
        a first RNA having a first label attached
        thereto and a second RNA, such first label
        being capable of producing a luminescent
        energy pattern when the first RNA is present
        in the RNA duplex which differs from the
        luminescent energy pattern produced when the
        first RNA is not present in the RNA duplex;

    b)  subjecting the admixture to conditions which
        permit (i) the RNA helicase to unwind the RNA
        duplex and release single-stranded RNA, and
        (ii) the first label to produce luminescent
        energy; and

    c)  detecting a change in the luminescent energy
        pattern produced by the first label so as to
        thereby detect release of single-stranded RNA
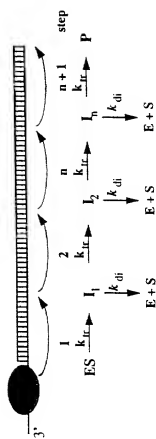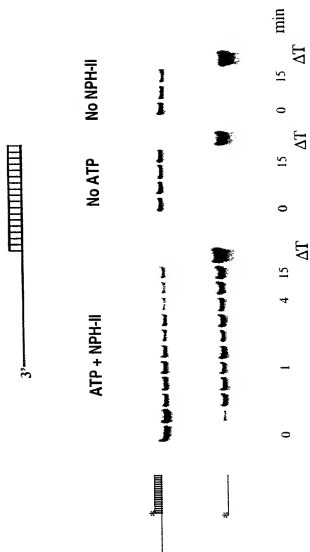        from the RNA duplex.

5.  The method of claim 1, wherein in step (a) the
    conditions which permit the RNA helicase to unwind
    the RNA duplex and release single-stranded RNA
    comprise the presence of ATP and a divalent cation.

6.  The method of claim 1, wherein the first label is
    present at the 5' end of the first RNA.

4.   The method of claim 1 or 3, wherein a second label
     is attached to the 3' end of the second RNA and the
     luminescent   energy   pattern   results   from   the
     interaction of luminescent energy released from the
     first label with the second label.

5.   The method of claim 4, wherein the first and second
     label comprise fluorophors and the second label
     absorbs luminescent energy released from the first
     fluorophor.

6.   The method of claim 5, wherein the first label is
     fluorescein iscothiocyanate and the second label is
     rhodamine isothiocyanate.

7.   A method of measuring the rate of release of a
     single-stranded RNA from an RNA duplex which
     comprises detecting whether the single-stranded RNA
     is released from the RNA duplex at predetermined
     time intervals according to the method of claim 1,
     and determining therefrom the rate of release of the
     single-stranded RNA from the RNA duplex.

8.   A method of determining whether a compound is
     capable of modulating the release of a single-
     stranded RNA from an RNA duplex by an RNA helicase
     which comprises detecting the release of the single-
     stranded RNA from the RNA duplex according to the
     method of claim 1, wherein the compound is added to
     the mixture of step (a).

## Assays For Evaluating
## The Function Of RNA Helicases

5

### Abstract of the Disclosure

The present invention provides a method for detecting the
release of a single-stranded RNA from an RNA duplex which
comprises admixing an RNA helicase with the RNA duplex
under conditions permitting the RNA helicase to unwind
10    the RNA duplex and release single-stranded RNA, wherein
the RNA duplex comprises a first RNA having a first label
attached thereto and a second RNA, such first label being
capable of producing a luminescent energy pattern when
the first RNA is present in the RNA duplex which differs
15    from the luminescent energy pattern produced when the
first RNA is not present in the RNA duplex, subjecting
the admixture to conditions which permit (i) the RNA
helicase to unwind the RNA duplex and release single-
stranded RNA, and (ii) the first label to produce
20    luminescent energy, and detecting a change in the
luminescent energy pattern produced by the first label so
as to thereby detect release of single-stranded RNA from
the RNA duplex.

FIGURE 1

step

**P**

$n+1$
$k_{fc}$

$\mathbf{I_n}$

$k_{di}$

$E + S$

$n$
$k_{fc}$
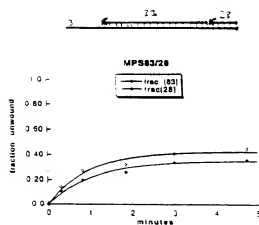
$\mathbf{I_2}$

$k_{di}$

$E + S$

$2$
$k_{fc}$

$\mathbf{I_1}$

$k_{di}$

$E + S$

$1$
$k_{fc}$

ES

3'

FIGURE 2

FIGURE 3

FIGURE 4



excitation
492 nm                                          excitation
                          unwinding               492 nm

fluorescence
energy
transfer

518 nm    580 nm                                 518 nm

fluorescence                                     fluorescence

wavelength                                        wavelength

18 bp duplex                                    36 bp duplex

fraction unwound                                fraction unwound

20  40  60  80  100  120                        20  40  60  80  100  120
        seconds                                          seconds
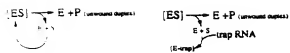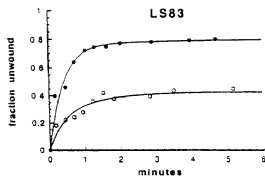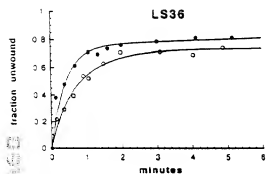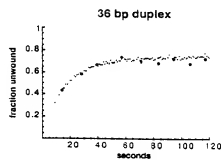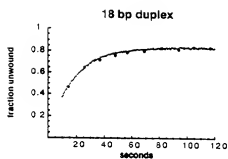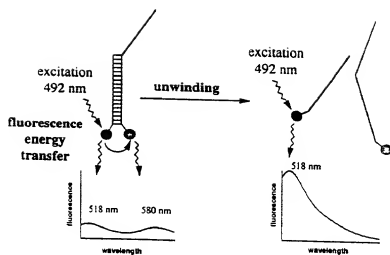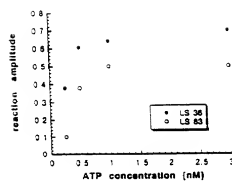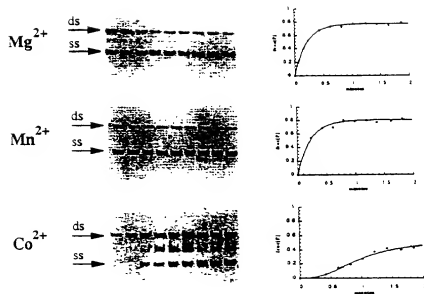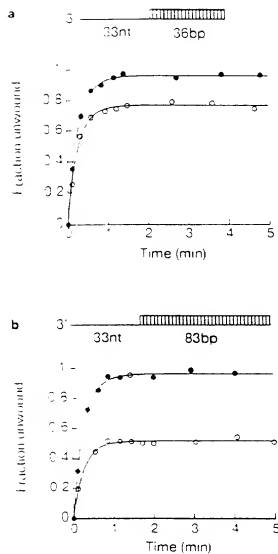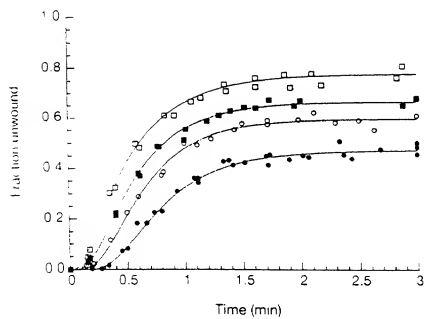
FIGURE 5

FIGURE 6

FIGURE 7
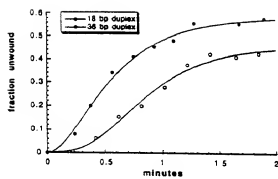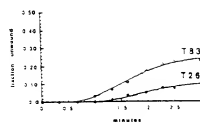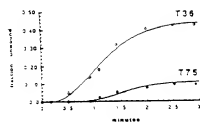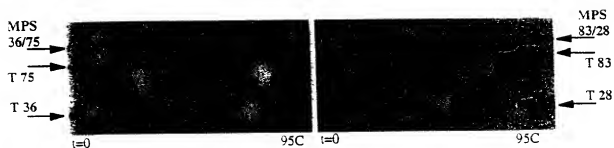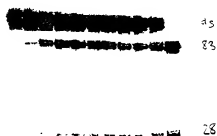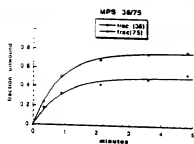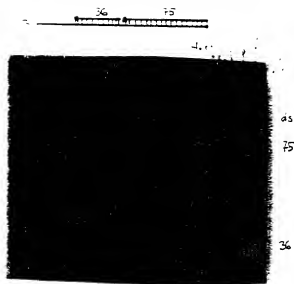
FIGURE 9

FIGURE 10

FIGURE 11

FIGURE 12

FIGURE 13